Tellus (2003), 55A, 173–180
Printed in UK. All rights reserved

TELLUS
ISSN 0280–6495

Wave and form drag: their relation in the linear gravity wave regime

By MARIA ATHANASSIADOU*, *Met Office, London Road, Bracknell, Berkshire RG12 2SZ, UK*

(Manuscript received 7 January 2002; in final form 21 November 2002)

ABSTRACT

The linear, asymptotic work of Belcher and Wood (Belcher, S. E. and Wood, N., 1996. *Q. J. R. Meteorol. Soc.* **122**, 863–902), for the surface pressure drag over orography of small amplitude, is revised and expanded. A new equation is obtained that incorporates the pressure drag due to gravity waves (wave drag) and pressure drag due to turbulence (form drag) and shows how these mechanisms operate together. In its general form, the equation is in the Fourier space and can be solved numerically for any orography. An analytical example is given for sinusoidal orography.

1. Introduction

The effect of the turbulent boundary layer on drag calculations for stably stratified flow over orography has been of interest for some time, i.e., Chimonas (1999) and references therein. The type of response when stable air flows over orography depends on the airflow characteristics as well as the dimensions of the orography, and is characterised, in general, by a number of non-dimensional parameters that describe the relative importance of inertia, buoyancy, non-linear effects, rotation etc. The basic parameter for the discussion in this paper is the Froude number based on the hill's width, $F = U/Na$. U and N are the wind and buoyancy frequency of the flow, respectively, and a is a characteristic horizontal scale of the hill that for a sinusoidal orography is related to wavelength by $\lambda = 2\pi a$. A schematic diagram of the basic flow regimes categorised by F is shown in Fig. 1. Although this view does not include Coriolis or non-linear effects, such an approach is consistent with the analysis of this work, where orography of gentle slope and horizontal dimensions up to a few tens of kilometres is considered.

With this point of view in mind, two main and somewhat distinct regimes are identified depending on whether $F < 1$ or $F > 1$. $F = 1$ corresponds to a pole in the equation that describes the flow response over orography, the Taylor–Goldstein equation [eq. (3) in the next section], and has effectively divided the scientific community into two somewhat distinctive groups. As a result, the problem of air flow over complex terrain has traditionally been approached from two opposite directions, depending primarily on the scale of the orography involved.

For typical winds and stratification, the $F > 1$ regime is associated with small mountains and hills. The vertical perturbations in this case are evanescent and gravity waves are not sustained. Very large numbers of F are equivalent to neutral flow. This is the boundary layer view or approach to the problem. In this case, neutrally stratified turbulent flow over small hills embedded within the boundary layer is usually considered, with extensions to moderately stable stratified flow.

On the other hand, a larger-scale point of view of the orography examines stably stratified flow over larger orography, i.e., mountains that penetrate the boundary layer. In this case, the effects of the boundary layer are usually either assumed negligible or enter through friction at the lower boundary without explicit consideration of the interaction. This is the $F < 1$ regime, where gravity waves are sustainable. The horizontal and vertical wavelengths of the waves relate to the

*e-mail: maria.athanassiadou@metoffice.com

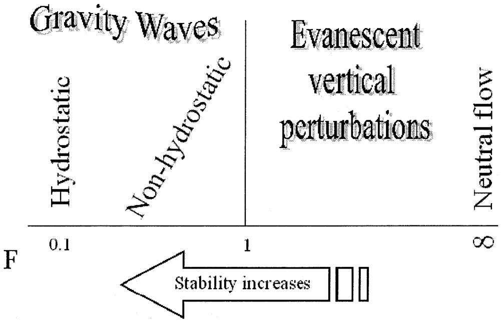

Fig. 1. Schematic diagram of flow regimes, categorised by F, the Froude number based on the horizontal dimensions of the orography.

orography that generates them, being proportional to $L_x \sim a$ and $L_z \sim (U/N)(1 - F^2)^{-1/2}$, respectively. When $F \ll 1$, $L_x \gg L_z$ and the gravity waves are hydrostatic, with all the wave energy confined above the orography. For larger values of F, but still $F < 1$, the waves have progressively smaller horizontal wavelengths and propagate downstream as well as upwards of the mountain.

It might be helpful at this point to briefly introduce some basic concepts to facilitate the discussion later in the paper. With any type of orographic flow, a force is felt on the mountain that has contributions from the integral over the mountain of (a) the tangential stress at the mountain's surface (acting in a direction parallel to the mountain's surface) and (b) the normal stress (acting perpendicular to the mountain's surface). The former acts in a direction opposite to that of the fluid and is termed friction drag, since it is wholly and directly a consequence of viscosity or internal friction of the fluid. The force due to the normal stress at the surface of a body has a more complex origin. It results from pressure differences over the surface of the mountain and is termed pressure drag [Massey (1989) and similar textbooks]. The total surface force per unit area can therefore be written:

$$F_{\mathrm{tot}} = F_\tau + \Delta F_{\mathrm{p}} = F_\tau + F_{\mathrm{p}} + F_{\mathrm{w}} \tag{1}$$

where $F_\tau = \rho_{\mathrm{s}} u_{*\mathrm{o}}^2$ is the friction stress and ΔF_{p} is the contribution due to surface pressure perturbations whose integral over the hill does not become zero. Pressure perturbations on the surface of the hill can arise due to different mechanisms and hence result in different types of drag, not always independent of one another. In principle, the surface pressure drag ΔF_{p} can further be decomposed into wave drag F_{w} and form drag F_{p}. The wave drag F_{w} is due to vertically propagating gravity waves that produce a surface pressure profile that is out of phase with the orography. This is an inviscid process. On the other hand, there is no F_{p} for inviscid flow. This is because the surface pressure profile, in the absence of gravity waves, is in phase with the orography (Durran, 1986), so any drag in this regime has to come from other mechanisms, i.e., flow separation, turbulence etc. In the linear regime, with no wakes or flow separation, the form drag F_{p} is due to turbulence, according to the sheltering mechanism of Belcher et al. (1993).

For inviscid flow in the gravity wave regime $F < 1$, $\Delta F_{\mathrm{p}} = F_{\mathrm{w}}$ only, whereas for turbulent, neutral or weakly stratified flow over hills with $F > 1$, $\Delta F_{\mathrm{p}} = F_{\mathrm{p}}$. The $F < 1$ regime therefore has traditionally been associated with larger orography, gravity waves and wave drag, while the $F > 1$ regime has been associated with small hills, turbulent flow and form drag. For turbulent, stratified flow in the $F < 1$ regime both wave and form drag mechanisms can, in principle, coexist, and examination of their relation is the scope of this paper.

It is important to appreciate one's view of the problem, because friction affects the flow differently, depending on the regime under consideration. From the large-scale point of view, the notion is that friction reduces the amplitude of the waves and suppresses wave breaking. This is true because studies in that area, Olafsson and Bougeault (1997) for example, concentrate in the non-linear regime where wave breaking occurs. The effects of turbulence in the linear wave regime ($F < 1$) have received less attention.

Approaching the problem from the smaller-scale, boundary layer view, Belcher and Wood (1996; BW hereafter), obtained an analytical formula for the pressure drag due to stably stratified turbulent flow over two-dimensional ridges of small slopes. They divided the flow into an inner and an outer region, with the outer region further subdivided into a middle and an upper layer. Appropriate scaling was applied on each layer. Solutions for the flow behaviour were sought in each layer, then matched across the layers. They showed that the perturbations to the flow and the surface pressure drag depended on whether $F < 1$ or $F > 1$, and that the appropriate height for the parameters' scaling was the middle layer height, h_{m}. For stable, turbulent flow in the $F > 1$ regime, BW showed that the same mechanism as for neutral flow leads to an asymmetry in the flow very close to the surface, resulting to form drag on the hill. The difference from neutral flow is that in stratified flows, the form drag varies with stratification. When $F < 1$, in the absence of turbulence and friction, the surface pressure drag is due solely to the gravity waves, whereas for stable turbulent flow, wave and form drag can coexist. The BW results suggest that in this case the form drag is negligible and the wave drag increases with increasing stability.

Weng et al. (1997), starting from the inviscid flow equations and constant U and N, obtained the same formula as BW for the $F < 1$ regime, with the free stream wind U replacing BW's U_{m}, the wind at middle layer height. The difference at first glance between eq. (54) of BW and eq. (34) of Weng et al. is because BW consider pressure drag per wavelength while the equation of Weng et al. is for the pressure drag. Weng et al. compared their equation with results from their mixed spectral finite-difference model and found that stratification and turbulence gives values very close to inviscid theory, for about $F \geq 0.6$. For $F < 0.6$, the difference between the analytic solution and the model increased with decreasing F.

In this work, the drag equation of BW is re-examined. Following the basic analysis of BW, the same expression is obtained for $F > 1$. For $F < 1$ though, the analysis of this work shows an extra term in the drag equation that sheds new light on the relation between wave and form drag in the gravity wave regime. Moreover, some results for flow over sinusoidal orography using the new equation might help to explain the differences in drag between theory and the numerical results observed by Weng et al. (1997), for small Froude numbers. The structure of the rest of this paper is as follows. Section 2 contains the relevant mathematical analysis. The new equation is discussed in Section 3, for flow over sinusoidal terrain. Moreover, some comparisons are made between the complete equation and the analytical inviscid solution that predicts only wave drag for $F < 1$. A summary is given in Section 4.

2. Mathematical formulation

In this work, only the parts of the analysis of BW that are essential for the derivation of the new equation are rewritten, since the purpose here is to reproduce only the necessary arguments and equations leading to the point of interest. For the full analysis and general discussion, the reader is referred to the original paper of BW. To facilitate the discussion though, the same notation as that of BW has been used as far as possible.

The BW analysis starts with an approaching flow, having the usual log-linear profiles, and flowing over gentle hills whose surface is described by some function $z = z_{\mathrm{s}}(x)$, Fig. 2. Perturbations to the mean flow are taken to be small and linear analysis is assumed. The dependent variables are expressed in their Fourier transforms, shown with a tilde, and are functions of height z and wavenumber k. A reference wind speed $U_{\mathrm{m}} = U(h_{\mathrm{m}})$ is defined as the wind speed in the approach flow at the middle layer height h_{m}.

The pressure perturbation is assumed constant with height to leading order across the inner region and equal to its surface value, thus from BW:

$$\Delta \tilde{p}(k, 0) = \rho_{\mathrm{s}} U_{\mathrm{m}}^2 \tilde{\sigma} \tag{2}$$

where $\tilde{\sigma}$ is a dimensionless coefficient.

In the outer region, the flow at leading order is described by the Taylor–Goldstein equation,

$$\frac{\mathrm{d}^2 \Delta \tilde{w}}{\mathrm{d}z^2} - \left(k^2 - \frac{N^2}{U^2} + \frac{U''}{U} \right) \Delta \tilde{w} = 0. \tag{3}$$

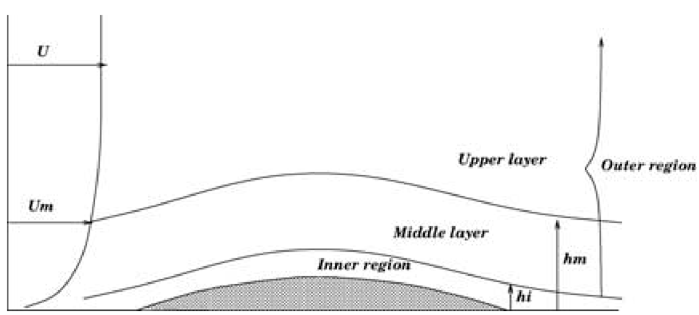

Fig. 2. Schematic diagram of the hill, approaching flow and the various regions.

In the upper layer, the curvature term U''/U is smaller than the other terms and eq. (3) becomes

$$\frac{\mathrm{d}^2\Delta\tilde{w}}{\mathrm{d}z^2} - k^2\left(1-\frac{N^2}{k^2U^2}\right)\Delta\tilde{w} = \frac{\mathrm{d}^2\Delta\tilde{w}}{\mathrm{d}z^2} - k^2\left(1-\frac{1}{F^2}\right) = 0. \tag{4}$$

The latter can be solved with the WKB method, provided that F varies slowly with height in the upper layer. The slowly varying wavenumber $-\mathrm{i}M$, depends on the sign of $Q(z) = 1 - 1/F^2$ in the following way:

$$M(z) = \begin{cases} -\,|k|\,|Q|^{1/2} & \text{for} \quad F > 1 \\ \mathrm{i}k\,|Q|^{1/2} & \text{for} \quad F < 1. \end{cases} \tag{5}$$

The signs are chosen to satisfy the boundary conditions at large z, i.e., when $F > 1$ the vertical velocity perturbation decays with height, whereas for $F < 1$ gravity waves are possible and a radiation upper boundary condition is assumed.

By matching the solutions across the regions, BW were able to evaluate the surface pressure coefficient $\tilde{\sigma}$ as:

$$\tilde{\sigma} = \tilde{z}_\mathrm{s}\frac{M_\mathrm{m}}{1-h_\mathrm{m}M_\mathrm{m}} + \mathrm{i}\,\frac{\tilde{z}_\mathrm{s}}{k}\,\frac{M_\mathrm{m}^2}{(1-h_\mathrm{m}M_\mathrm{m})^2}\,\frac{4\epsilon^2}{\gamma^4} + \text{s.r.t.} + \text{s.i.t.} \tag{6}$$

where s.r.t. = smaller real terms, s.i.t. = smaller imaginary terms, $\epsilon = u_*/U_\mathrm{m}$, u_* being the friction velocity, and $\gamma^{-1} = [U_\mathrm{m}/U_{h\mathrm{i}}]$, $U_{h\mathrm{i}}$ being the velocity at the inner layer height h_i.

Equation (6) above, which is the same as eq. (40) of BW, shows that the Fourier transform of the surface pressure always has an imaginary part, and hence the pressure at the surface of the hill has a component that is asymmetric with the hill and leads to pressure drag. The magnitude of the dimensionless pressure coefficient $\tilde{\sigma}$ is determined by the value of M_m, i.e., M at the middle height h_m, which in turn depends on whether $F > 1$ or $F < 1$.

In BW the terms $O(h_\mathrm{m}M_\mathrm{m})$ are neglected, and eq. (6) is simplified to:

$$\tilde{\sigma} = \tilde{z}_\mathrm{s}M_\mathrm{m} + \mathrm{i}\frac{\tilde{z}_\mathrm{s}}{k}M_\mathrm{m}^2\frac{4\epsilon^2}{\gamma^4}. \tag{7}$$

Substitution of $\tilde{\sigma}$ from eq. (7) to eq. (2) gives the Fourier transform of the surface pressure perturbation as:

$$\Delta\tilde{p}(k,0) = \rho_\mathrm{s}U_\mathrm{m}^2\tilde{z}_\mathrm{s}M_\mathrm{m} + \mathrm{i}\rho_\mathrm{s}U_\mathrm{m}^2\,\frac{\tilde{z}_\mathrm{s}}{k}M_\mathrm{m}^2\,\frac{4\epsilon^2}{\gamma^4}. \tag{8}$$

2.1. F > *1 regime*

In this case

$$M_\mathrm{m} = -\,|k|\,|Q|^{1/2} = -\,|k|\left(1-\frac{1}{F^2}\right)^{1/2} \tag{9}$$

and

$$M_\mathrm{m}^2 = k^2\left(1-\frac{1}{F^2}\right). \tag{10}$$

Substitution of eqs. (9) and (10) in eq. (8) gives the Fourier transform of the surface pressure perturbation in this case as:

$$\Delta\tilde{p}(k,0) = -\rho_\mathrm{s}U_\mathrm{m}^2\tilde{z}_\mathrm{s}k\left(1-\frac{1}{F^2}\right)^{1/2} + \mathrm{i}\rho_\mathrm{s}U_\mathrm{m}^2\tilde{z}_\mathrm{s}k\left(1-\frac{1}{F^2}\right)\frac{4\epsilon^2}{\gamma^4}. \tag{11}$$

The part of the surface pressure that will account for the pressure drag is the imaginary part of eq. (11), form drag only in this case. Equation (11) is the same as eq. (41) of BW for $F > 1$.

2.2. F < *1 regime*

In this case

$$M_\mathrm{m} = \mathrm{i}k\,|Q|^{1/2} = \mathrm{i}k\left(\frac{1}{F^2}-1\right)^{1/2} \tag{12}$$

and

$$M_\mathrm{m}^2 = -k^2\left(\frac{1}{F^2}-1\right). \tag{13}$$

Now, substitution of eqs. (12) and (13) in eq. (8) gives:

$$\Delta\tilde{p}(k,0) = \mathrm{i}k\rho_\mathrm{s}U_\mathrm{m}^2\tilde{z}_\mathrm{s}\left(\frac{1}{F^2}-1\right)^{1/2} - \mathrm{i}k\rho_\mathrm{s}U_\mathrm{m}^2\tilde{z}_\mathrm{s}\left(\frac{1}{F^2}-1\right)\frac{4\epsilon^2}{\gamma^4}. \tag{14}$$

In this case, both terms in eq. (14) are imaginary and will contribute to the surface pressure drag. The first term in eq. (14) is the same as eq. (41) of BW for $F < 1$. The second term in eq. (14) is the same as the imaginary part of eq. (11) for $F > 1$, but with the opposite sign. This second term is the one overlooked in the final analysis of BW, eq. (41) for $F < 1$.

Equation (14) is the fundamental contribution of this work. It shows the relationship between wave drag and form drag and describes the way these two drag mechanisms operate together in the wave regime. Equation (14) will be discussed in more detail in Section 3.

Furthermore, to facilitate the physical discussion of the new equation, the surface pressure drag is evaluated for sinusoidal terrain. This also enables direct comparison with part of the analysis of BW and also with the results of Weng et al. (1997).

3. Drag on sinusoidal terrain

In this case the terrain profile is simply given by $z_s = h\Re\{e^{ikx}\} = h \cos(kx)$, where h is the maximum amplitude of the hills, and k the wavenumber. To facilitate the derivation, eqs. (11) and (14) are written in more concise forms, defining

$$\mathcal{A} \equiv \rho_s \,|Q|\, 4u_*^2 \left(\frac{U_m}{U_{hi}}\right)^4 \tag{15}$$

and using the definitions of ϵ and γ given previously.

3.1. F > 1 regime

Equation (11) is rewritten, using eq. (15), as

$$\Delta\tilde{p}(k,0) = -\rho_s U_m^2 \,|Q|^{1/2}\, k\tilde{z}_s + ik\tilde{z}_s\mathcal{A} \tag{16}$$

and the pressure perturbation at the surface of the hill is obtained from

$$\Delta p(x,0) = -\mathcal{A}\, kh \sin(kx). \tag{17}$$

The surface pressure force per wavelength $\lambda = 2\pi/k$ is then given by

$$\Delta F_p = \frac{1}{\lambda}\int_0^{\lambda} \Delta p(x,0)\frac{dz_s}{dx}dx \tag{18}$$

which, using eq. (17), becomes:

$$\Delta F_p = \frac{1}{2}\mathcal{A}k^2h^2 \tag{19}$$

or

$$\Delta F_p = k^2h^2\rho_s\left(1-\frac{1}{F^2}\right)2u_*^2\left(\frac{U_m}{U_{hi}}\right)^4. \tag{20}$$

This is the same as eq. (54) of BW for sinusoidal terrain in the $F > 1$ regime.

3.2. F < 1 regime

In this case, we get from eq. (14) and using eq. (15),

$$\Delta\tilde{p}(k,0) = \rho_s U_m^2 \,|Q|^{1/2}\, ik\tilde{z}_s - ik\tilde{z}_s\mathcal{A}, \tag{21}$$

and the surface pressure perturbation is obtained for this regime from

$$\Delta p(x,0) = -\rho_s U_m^2 \,|Q|^{1/2}\, hk \sin(kx) + \mathcal{A}hk \sin(kx). \tag{22}$$

The surface pressure drag is then

$$\begin{aligned}\Delta F_p &= \frac{k}{2\pi}\int_0^{2\pi/k} \rho_s U_m^2 \,|Q|^{1/2}\, h^2k^2 \sin^2(kx)\,dx \\ &\quad - \frac{k}{2\pi}\int_0^{2\pi/k} \mathcal{A}k^2h^2 \sin^2(kx)\,dx \\ &= \frac{1}{2}\rho_s U_m^2 \,|Q|^{1/2}\, h^2k^2 - \frac{h^2k^2\mathcal{A}}{2}\end{aligned}$$

or

$$\begin{aligned}\Delta F_p &= h^2k^2\rho_s U_m^2 \frac{1}{2}\left(\frac{1}{F^2}-1\right)^{1/2} \\ &\quad - h^2k^2\rho_s\left(\frac{1}{F^2}-1\right)2u_*^2\left(\frac{U_m}{U_{hi}}\right)^4.\end{aligned} \tag{23}$$

This is the analogue of eq. (54) of BW for the $F < 1$ regime. The difference between eq. (23) above and eq. (54) of BW is the second term in eq. (23). This is the form drag contribution to the total surface drag in the gravity wave regime, for flow over sinusoidal terrain. The first term is also the same as the Weng et al. (1997) equation, with U replacing U_m. Not surprisingly, the equation of Weng et al. (1997) does not have a second term, since their analysis excludes the effects of turbulence and therefore form drag.

We now proceed to discuss the new equation in more detail. To do that, we define a drag coefficient A_m,

$$A_m = \frac{\Delta F_p}{h^2k^2\rho_s U_m^2} = \frac{\Delta F_p}{\sigma^2\rho_s U_m^2} \tag{24}$$

where $\sigma = hk$ is the maximum slope for sinusoidal terrain. The surface pressure drag is scaled by the same factor for both $F < 1$ and $F > 1$. Moreover, it should be kept in mind that the scaling velocity U_m, is the same as the free stream velocity when the middle layer height is greater than the boundary layer depth, z_i, defined here as the height where the Reynolds stress is an order of magnitude less than its surface value. Equations (20) and (23) are then written:

$$A_{\rm m} = \begin{cases} \left(1-\frac{1}{F^2}\right)2\left(\frac{u_*}{U_{\rm m}}\right)^2\left(\frac{U_{\rm m}}{U_{h{\rm i}}}\right)^4; & F>1 \\ \underbrace{\frac{1}{2}\left(\frac{1}{F^2}-1\right)^{1/2}}_{C_1} + \underbrace{\left(1-\frac{1}{F^2}\right)2\left(\frac{u_*}{U_{\rm m}}\right)^2\left(\frac{U_{\rm m}}{U_{hi}}\right)^4}_{C_2}; & F<1 \end{cases} \tag{25}$$

For $F > 1$, $A_{\rm m}$ is similar to the sheltering coefficient α of BW, except for the $(u_*/U_{\rm m})^2$ term, due to the fact that the scaling velocity in BW is u_* in this regime. The expression for the form drag is the same to that for neutral flow, apart from the additional presence of the $(1 - 1/F^2)$ factor.

For $F < 1$, $A_{\rm m}$ consists of two parts which in the following discussion will be termed C_1 and C_2 for convenience. C_1 is the formula for inviscid flow, and gives the normalised wave drag on the hill due to propagating gravity waves. With decreasing stratification, i.e., increasing Froude number, C_1 decreases monotonically [Fig. 6 of Weng et al. (1997)]. The second term, C_2, is the contribution of the form drag in the wave regime. It acts in the opposite sense to the wave drag, i.e., the two mechanisms oppose each other. Note that C_2 as defined by eq. (25b) has the same form as the drag coefficient $A_{\rm m}$ for $F > 1$, but is negative for $F < 1$ whereas it is positive for $F > 1$. Moreover, as $u_* \to 0$, the C_2 term decreases and the main contribution is from the first term, C_1. For $u_* = 0$, the inviscid result, C_1 only is recovered.

The quantitative contribution of C_2 is not obvious straight away: in particular, the behaviour of the shear factor $(U_{\rm m}/U_{hi})^4$ in C_2 needs more examination. To assess its magnitude with varying F, realistic profiles of U and N were obtained, using the numerical model BLASIUS, described in BW, to grow boundary layer profiles over a range of hills, covering typical Froude numbers in the range of interest. These are summarised in Table 1, along with the relevant parameters.

The maximum slope of the hills is equal to $\sigma = 0.025$ in the $F < 1$ regime and $\sigma = 0.03$ for $F > 1$, so that linear theory is applicable. The roughness length $z_{\rm o} = 0.1$ m in all cases. The Froude number is changed by varying the wavelength of the hills, while keeping the wind and stratification the same, i.e., the free stream velocity is $U = 10$ m s^{-1} and $N = 10^{-2}$ s^{-1}. The normalised vertical surface buoyancy flux is zero for the $F < 1$ simulations and equal to -0.0005 m^2 s^{-3} for $F > 1$. The inner layer height, $h_{\rm i}$, is obtained from $kh_{\rm i}\, U(h_{\rm i})/u_* = 2\kappa$, consistent with BW. The von Kármán constant, κ, is taken equal to 0.4. In all simulations the middle layer height $h_{\rm m}$ was obtained, following BW, from

$$1 - \frac{N^2}{k^2U^2} = -\frac{1}{k^2U}\frac{{\rm d}^2U}{{\rm d}z^2} \tag{26}$$

and ensuring that $|(1/U)({\rm d}^2U/{\rm d}z^2)| \ll |k^2 - N^2/U^2|$ in the outer region.

For the cases in the wave regime $F < 1$, the upper layer lies entirely above the boundary layer, and, consistent with BW, $h_{\rm m}$ is set equal to $z_{\rm i}$. For those particular cases, it is found that the shear factor $(U_{\rm m}/U_{hi})^4$ increases with increasing F, the change being less than 15% as F varies from 0.1 to 0.7 (Table 1). Moreover, the $(u_*/U_m)^2$ factor does not change much with F and is approximately 2.3×10^{-3} for the examples considered here. Thus the combined effect of the friction and shear factors is $O(0.01)$ and as a result, C_2 has the greatest contribution for small Froude

Table 1. *Summary of simulations and relevant parameters*[a]

Run	F	λ	h	$z_{\rm i}$	C_1	C_2	C_2/C_1	$A_{\rm m}$	F-F	S-F	$h_{\rm m}$	$h_{\rm i}$
R100	0.1	63000	500	1000	4.975	−1.67	33%	3.305	2.396	3.52	1000	525
R200	0.2	31416	250	800	2.45	−0.38	15 %	2.07	2.2	3.6	800	237
R400	0.4	16000	125	700	1.146	−0.09	8%	1.06	2.257	3.805	700	135
R625	0.625	10053	80	675	0.624	−0.028	4%	0.6	2.19	4.165	675	84
R703	1.43	3000	30	340	0	0.019	N/A	0.019	2.604	7.2	143	31
R702	2.	2000	20	330	0	0.034	N/A	0.034	2.991	7.59	115	23
R701	3.15	1000	10	310	0	0.048	N/A	0.048	4.088	6.525	67	13

[a]F-F $= (u_*/U_{\rm m})^2$ is the friction factor. The values shown are $\times 10^{-3}$. S-F $= (U_{\rm m}/U_{hi})^4$ is the shear factor. Values of λ, h, $z_{\rm i}$, $h_{\rm m}$ and $h_{\rm i}$ are in m.

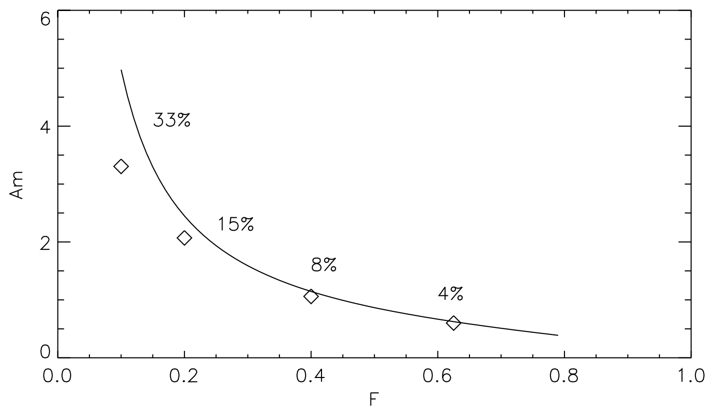

Fig. 3. Drag coefficient as a function of Froude number in the wave regime. The solid line represents the inviscid solution; diamonds are for eq. (25b). Details of the simulations are shown in Table 1.

numbers, where the stratification factor Q has the strongest effect.

Figure 3 shows the drag coefficient A_{m} as a function of the Froude number. The solid line is the inviscid solution, term C_1 only, and shows the decrease of normalised wave drag with increasing F, for $F < 1$. The diamonds are for A_{m} from eq. (25b), with a contribution from both terms C_1 and C_2. For $F \geq 0.6$, there is little difference between the complete eq. (25b) and inviscid theory. For smaller Froude numbers the difference increases with decreasing F. The percentage of the difference between C_2 and C_1 is also shown in Fig. 3. There is rather good agreement with Weng et al. (1997), who also observed similar behaviour between their model results and inviscid theory and who found that in the wave regime, for weak to moderate stratification, there is little difference between the drag obtained for turbulent flow and for inviscid flow, although the flow itself can be quite different between the two cases.

Figure 4 shows C_2 only, as a function of F, on a log-linear plot. For $F > 1$, C_2 is identical to A_{m}. Moreover, as also can be seen from Table 1, C_2 is an order or two larger in the wave regime than for $F > 1$. As a result, the plot is focused around Froude number unity, to better illustrate the transition of the form drag between the $F < 1$ and $F > 1$ regimes. As is also apparent from Table 1, C_2 increases rapidly with increasing F in the wave regime, whereas for $F > 1$, the increase is more gradual. Because there is no inviscid drag for $F > 1$, turbulence has a positive overall effect there. On the other hand, wave drag is maximum for inviscid flow

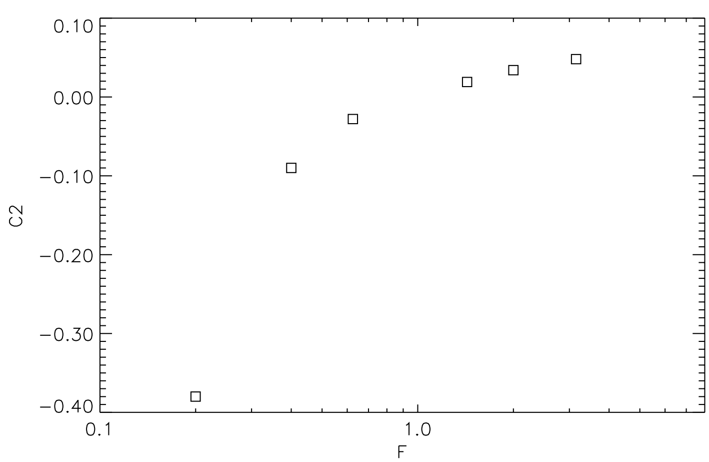

Fig. 4. Normalised form drag part of the drag coefficient as a function of Froude number from eqs. (25a) and (25b).

and is reduced by turbulence, which has a negative contribution to the drag in this regime.

Weng et al. (1997) showed that for turbulent flow in the $F < 1$ regime, the pressure drag decreases with increasing roughness. Equation (25b) shows exactly how this is achieved. The increase in surface roughness results in C_2 being larger than for a smoother surface, and as a result to even less drag than the inviscid prediction, term C_1 alone.

One final remark relates to the applicability of the analysis here, for small Froude numbers. At some point in the analysis, we neglect the terms $h_\mathrm{m} M_\mathrm{m}$ from eq. (6). In the original analysis of BW, this was done because they were considered the same order of magnitude as $O(kh_\mathrm{m})$, which in turn was $O(\epsilon^{1/2})$ and therefore small. In the wave regime, the terms $O(h_\mathrm{m} M_\mathrm{m})$ can also be left out, with the following argument. For $F = Uk/N < 1$, $N^2/U^2 \gg k^2$ and $h_\mathrm{m} M_\mathrm{m} \sim h_\mathrm{m} N_\mathrm{m}/U_\mathrm{m}$, which is indeed small in the cases examined. N, U and N_m, U_m are used interchangeably here, since $h_\mathrm{m} = z_\mathrm{i}$ in these cases.

4. Summary

BW used linear analysis to examine stably stratified flow over low ridges and derived a dimensionless surface pressure coefficient. Later in their analysis, they dropped a term that represents the effect of turbulence on the drag in the wave regime. Here, this term is retained and its effect on the overall surface drag in the wave regime is examined. It predicts the reduction of surface pressure drag from its inviscid value, as a function of Froude number. The new equation shows how the drag mechanisms due to gravity waves and turbulence operate together in the wave regime, Froude number $F < 1$. In its general form in the Fourier space, eq. (14) can be used very easily to numerically compute the drag over an arbitrary terrain of low slope. An analytical example was given for sinusoidal terrain and the results compared well with previous work of BW for $F > 1$ and the numerical results of Weng et al. (1997). In particular, it was shown how turbulence changes the surface drag from its inviscid value and the way this change depends on stability.

Surface pressure drag always exists due to turbulence. On the other hand, turbulence has a different effect on the surface pressure drag in the two regimes. For inviscid flow in the $F > 1$ regime, there is no surface pressure drag because the surface pressure profile is 180° out of phase with the orography, with the maximum over the trough and minimum over the crest. In this case, as is known from Belcher et al. (1993), turbulence moves the surface pressure out of anti-phase and to the right with respect to the hill, resulting in surface pressure drag on the hill, form drag in this case. For $F < 1$, the maximum surface pressure drag is obtained for inviscid flow where the surface pressure shift is 90° out of phase with the orography, with high pressure over the upwind slope and minimum in the lee. The effect of turbulence in this case is to reduce this optimum surface pressure shift by moving the surface pressure out of phase and to the right with respect to the orography, the same way it did for $F > 1$. Equation (25) shows how turbulence achieves this in the wave regime.

The analysis here, of the wave and form drag co-existence, is by no means exhaustive and although other factors, such as non-linearities and three-dimensional effects, might be important in general, the equation of the present analysis represents, within the limits of its applicability, a step towards a unified approach between the thus far, distinct worlds of wave and form drag.

5. Acknowledgements

The author thanks Andy Brown and Nigel Wood from the Met Office for their comments.

REFERENCES

Belcher, S. E., Newley, T. M. J. and Hunt, J. C. R. 1993. The drag on an undulating surface induced by the flow of a turbulent boundary layer. *J. Fluid Mech.* **249**, 557–596.

Belcher, S. E. and Wood, N. 1996. Form and wave drag due to stably stratified turbulent flow over low ridges. *Q. J. R. Meteorol. Soc.* **122**, 863–902.

Chimonas, G. 1999. Steps,waves and turbulence in the stably stratified planetary boundary layer. *Boundary-Layer Meteorol.* **90**, 397–421.

Durran, D. R., 1986. Mountain waves. In: *Mesoscale meteorology and forecasting* (ed. P. S. Ray). Am. Meteorol. Soc., 472–492.

Massey, B. S. 1989. *Mechanics of fluids*, 6th ed. Chapman and Hall, New York, 599 pp.

Olafsson, H. and Bougeault, P. 1997. The effect of rotation and surface friction on orographic drag, *J. Atmos. Sci.* **57**, 193–210.

Weng, W., Chan, L., Taylor, P. A. and Xu, D. 1997. Modelling stably stratified boundary-layer flow over low hills. *Q. J. R. Meteorol. Soc.* **123**, 1841–1866.